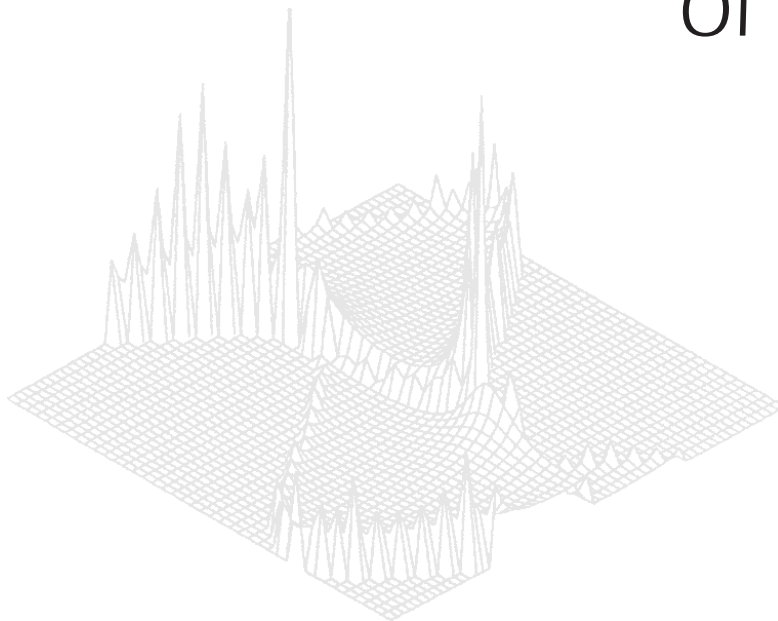

CSIRO PUBLISHING

Australian Journal of Physics

Volume 51, 1998
© CSIRO 1998



A journal for the publication of
original research in all branches of physics

www.publish.csiro.au/journals/ajp

All enquiries and manuscripts should be directed to

Australian Journal of Physics

CSIRO PUBLISHING

PO Box 1139 (150 Oxford St)

Collingwood

Vic. 3066

Australia

Telephone: 61 3 9662 7626

Facsimile: 61 3 9662 7611

Email: peter.robertson@publish.csiro.au



Published by **CSIRO PUBLISHING**
for CSIRO and the
Australian Academy of Science



Studies of the Electron-impact Double-ionisation Process in Magnesium using Coincidence Techniques*

M. J. Ford

Department of Chemistry and Biochemistry, University of Maryland,
College Park, MD 20742, USA.

Present address: Electronic Structure of Materials Centre,
Physics Department, Flinders University of South Australia,
GPO Box 2100, Adelaide, SA 5001, Australia.

Abstract

This article will review recent measurements of the electron-impact double-ionisation of atomic magnesium. Results for the resonant Auger double-ionisation process with coincident detection of all three outgoing electrons, the (e,3e) experiment, and for the direct double-ionisation process where only two outgoing electrons are detected, the (e,(3-1)e) experiment, will be discussed. The results are analysed with reference to ionisation mechanisms and comparisons are made with calculated double-ionisation cross sections.

1. Introduction

Simultaneous detection of the momenta of the three outgoing electrons following electron-impact double-ionisation of an atomic target, the (e,3e) process, completely specifies the kinematics of the collision. Measurements of this kind can provide information on several aspects of the many-body problem including the interaction between the incident electron and target, the interactions between the products, and the mechanisms of double-ionisation. Once the mechanism of ionisation is understood, the (e,3e) process can be used to probe an even more fundamental problem of atomic dynamics, that of electron correlation in the target atom. With this ultimate aim in mind, we have initiated a research program at the University of Maryland and Johns Hopkins University to investigate double-ionisation of the magnesium atom. We have chosen magnesium as a target for the following reasons: it is a two-electron-like atom (two 3s electrons outside closed shells) that can be expected to exhibit a large amount of ground state correlation (Pascual *et al.* 1988), and the first excited state of the residual doubly-charged magnesium ion is well separated in energy from the ground state by 52.8 eV. In addition, double-ionisation via the $L_{2,3}M_1M_1$ Auger process occurs with a large probability in Mg and has allowed us to investigate resonant double-ionisation as well as non-resonant, or direct, double-ionisation mechanisms.

The cross section for electron impact double-ionisation is ninefold differential in the energies and angles of the outgoing electrons. The variables required to describe the process are shown in the vector diagram of Fig. 1 for an incident electron with energy E_0 and momentum vector \mathbf{p}_0 , a scattered electron with energy E_s

* Dedicated to Professor Erich Weigold on the occasion of his sixtieth birthday.

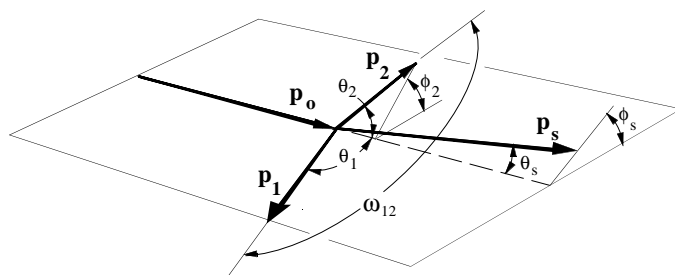


Fig. 1. Vector diagram for electron-impact double-ionisation with incident-electron momentum \mathbf{p}_0 , scattered-electron momentum \mathbf{p}_s , and ejected-electron momenta \mathbf{p}_1 and \mathbf{p}_2 . The reference plane is defined by the incident-electron momentum vector and one ejected-electron momentum vector so that the polar angle ϕ_1 is zero.

and momentum vector \mathbf{p}_s , and two ejected electrons with energies E_1 and E_2 and momentum vectors \mathbf{p}_1 and \mathbf{p}_2 . The first, fully differential, direct double-ionisation experiments were carried out by Lahmam-Bennani and co-workers on rare-gas targets (Lahmam-Bennani *et al.* 1989, 1992; Lahmam-Bennani and Duguet 1991). We have made similar (e, 3e) measurements of the double-ionisation of magnesium through the resonant Auger process (Ford *et al.* 1995*a*). These experiments were performed in the dipole scattering regime in which the scattering angle is small, so that the momentum transferred to the target by the incident electron is near the minimum required to eject two target electrons of the chosen energies. Under these conditions the results are expected to be similar to that observed for double-ionisation by photoabsorption (for example Kammerling and Schmidt 1991) since the electron-impact-ionisation cross section converges on the photoionisation cross section in the limit of zero momentum transfer (Inokuti 1971). Measurement of the angular correlation between ejected and Auger electrons can probe the effects of alignment of the ion-core following creation of the core-hole and provide a rigorous test of models of Auger emission. Angular correlations have been measured in photoionisation experiments by Kammerling and Schmidt (1991), however electron-impact measurements were previously restricted to simultaneous detection of the scattered electron and either ejected or Auger electron (Sandner and Volkel 1984; Sewell and Crowe 1984; Stefani *et al.* 1986).

By contrast to the Auger process, the cross section for direct double-ionisation is extremely small. A complete set of (e, 3e) measurements over a wide range of the independent variables would require prohibitively long data collection times. We (Ford *et al.* 1996, 1998) and Lahmam-Bennani and co-workers (El-Marji *et al.* 1996*a*, 1996*b*) have turned our attention to performing measurements in which only two ejected electrons are detected at fixed energies, thus effectively integrating the fully-differential cross section over the angles and energies of the other electron [these measurements are commonly referred to as (e, (3-1)e) experiments]. Because of this simplification, the momentum transferred by the incident electron in the collision is not known directly. Information regarding the ionisation mechanism can still be extracted from these measurements and they provide us with a guide in choosing appropriate conditions under which to perform the full (e, 3e) measurement.

In this paper I will describe our recent $(e, 3e)$ measurements of resonant double-ionisation and $(e, (3-1)e)$ measurements of direct double-ionisation of magnesium.

2. Experiment

A schematic diagram of the spectrometer is shown in Fig. 2 and a detailed description of the apparatus can be found in Ford *et al.* (1995*b*). The well-collimated monochromatic incident-electron beam is produced from a cathode-ray-tube type electron gun and intersects, at right angles, a jet of magnesium atoms produced by a resistively heated oven. The electron energy can be varied from 100 eV to 10 keV with an energy resolution of approximately 0.6 eV and beam currents of up to 10 μ A. The magnesium oven is operated at a temperature of approximately 620°C corresponding to a pressure of approximately 1 Torr.

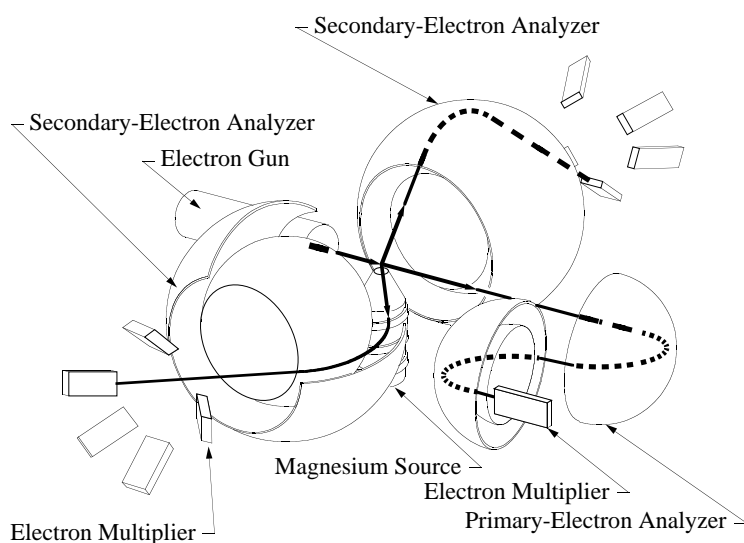


Fig. 2. Schematic diagram of the spectrometer. An $(e, 3e)$ event produces a signal at the primary analyser electron multiplier and two of the secondary analyser electron multipliers.

Scattered incident electrons falling within a solid angle of 2×10^{-4} sr around a scattering angle of $\theta_s = 0^\circ$ are decelerated by a factor of about 17 and are energy selected with a hemispherical electrostatic analyser (the primary-electron analyser). The decelerating lens system is not shown in the schematic diagram. Transmitted electrons are detected with a single-channel electron multiplier. The primary analyser is typically operated at an energy resolution of 4 eV. In the case of the $(e, (3-1)e)$ measurements the primary analyser is not operated.

Ejected electrons are energy selected with a pair of doubly truncated spherical electrostatic analysers (the secondary-electron analysers) located on opposite sides of the scattering volume on an axis perpendicular to the incident electron direction. The secondary analysers accept electrons ejected along the surfaces of a right circular cone whose apex is at the collision centre as shown in Fig. 3. The output of each secondary analyser can contain up to eight electron multipliers,

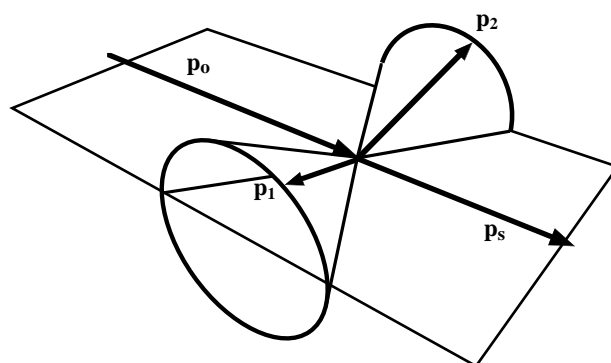


Fig. 3. Detection geometry of the spectrometer. Ejected electrons are detected along the surfaces of the right cone, either on the same side or opposite sides of the collision centre. The scattered electron is detected within a small solid angle at zero degree scattering angle.

the position of each multiplier defines the angle of emission of the ejected electron within a solid angle of about 0.04 sr. This allows us to sample up to 64 different pairs of ejection angles in a single experiment. With this geometry we can measure the cross section for θ_1 and θ_2 in the range 45° to 135° , and ϕ_2 in the range 0° to 90° . In the normal, 'opposite side' mode electrons enter the two secondary analysers on opposite sides of the collision centre, and the included angle, ω_{12} , between the two ejected-electrons is in the range 90° – 180° . A second configuration, the 'same-side' mode where both ejected electrons enter the same secondary analyser, gives $30^\circ < \omega_{12} < 90^\circ$, where θ_1 and θ_2 vary from 45° to 135° as before, and ϕ_2 varies from 90° to 180° . The secondary analysers are operated at a typical energy resolution of approximately 4 eV.

The outputs of the three (or two) electron analysers are fed to a CAMAC based data acquisition system controlled by a PC computer. As well as logging in which pair of secondary detectors the event has occurred, the arrival time difference of the three (or two) electrons at the detectors is also measured—commonly referred to as coincidence detection. A three (or two) dimensional time spectrum is thus accumulated for each set of detectors, electrons originating from a single collision event will be highly correlated in time and give rise to a peak in the timing spectrum allowing the desired double-ionisation events to be extracted from a large background of random events.

The geometry of our experiment is very different from the conventional planar geometry in which all of the detectors lie in a common plane that contains the incident-electron momentum vector. Our experiment has the advantage of wide angular coverage and capability of measuring cross sections both as a function of the included angle between the ejected-electron momentum vectors and as a function of the orientation of these vectors with respect to the incident-electron direction. These are particularly useful features in studies of the relation between the cross section and the kinematics of the collision. As a consequence of the wide angular range, detector coverage is rather sparse. The geometry of the apparatus means that certain sets of independent variables are sampled by more than one combination of detectors, and together with measurements of the Auger

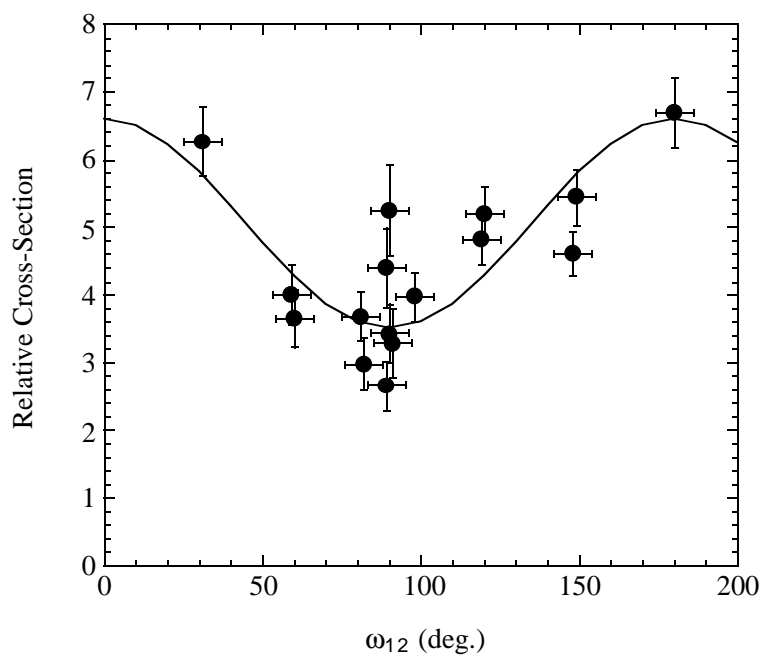


Fig. 4. Relative cross section for emission of two 35 eV electrons as a function of the included angle ω_{12} between the two electrons.

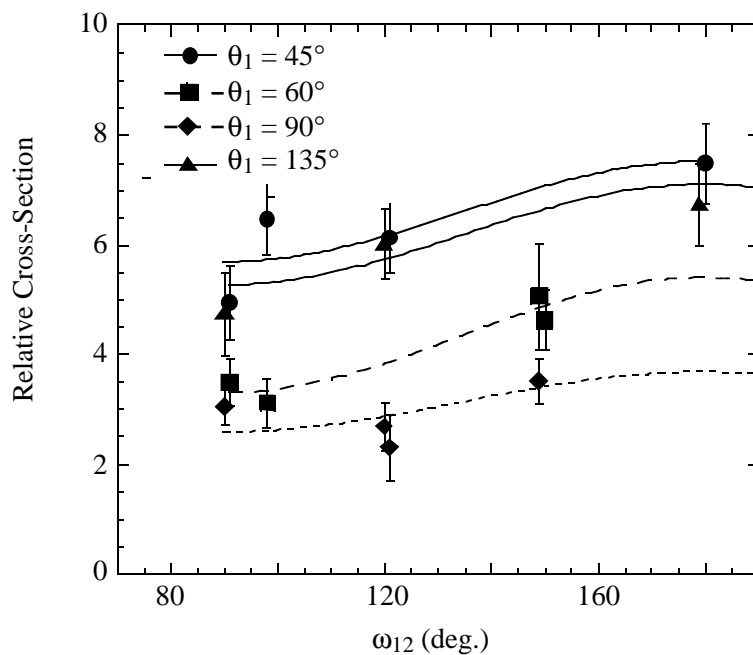


Fig. 5. Relative cross section for the ejection of a 45 eV electron and emission of a 35 eV Auger electron as a function of the included angle ω_{12} between the two electrons. The data are labelled according to θ_1 , the angle of the ejected electron with respect to the incident-electron direction.

cross section this provides an important check of instrumental variations due to differing detector efficiencies or misalignments; no such effects were observed.

3. (e, 3e) Measurements of Resonant Double-ionisation

The Mg $L_{2,3}M_1M_1$ Auger process proceeds by ejection of a 2p electron, an outer-shell 3s electron then fills this core-hole and the residual internal energy of the single ion gives rise to ejection of the other 3s electron at the characteristic Auger energy. There are two possible core-hole states, $2p_{1/2}$ and $2p_{3/2}$ giving rise to an Auger doublet with energies of 34.86 eV and 35.13 eV. The joint resolution of the apparatus is not sufficient to separate these two components, but is sufficient to distinguish the ground state of the double ion from all excited states.

We have performed a series of (e, 3e) measurements of the Auger transition at an impact energy of 3.5 keV (Ford *et al.* 1995a). Two secondary electrons are detected at angles between 45° and 135° with respect to the incident electron direction, one at the Auger energy of 35 eV, and one with an energy of either 100, 45 or 35 eV. The energy of the scattered electron is chosen to select events corresponding to the Mg double-ion being left in its ground state. The scattered electron is detected in a small solid angle around zero degree scattering angle. The energy and angular resolution of the scattered analyser means that the momentum transfer in the initial ionisation process cannot exceed 0.29 a.u.

Three independent angular variables are required to specify the measured cross section, for example θ_1 , θ_2 and ϕ_2 , and so there is no simple way of plotting the cross sections with respect to all the independent variables. For the case of equal-energy, 35 eV, secondary electrons, in which case the Auger and ejected 2p electron cannot be distinguished, the measured relative cross section appears to be a strong function of only the included angle ω_{12} , as shown in Fig. 4. The curve in Fig. 4 is a linear function of $\cos^2\omega_{12}$ and is only to guide the eye. It is interesting to note that the cross section is large for both small and large values of ω_{12} and is small near 90° . This result implies that Coulombic repulsion between the two outgoing secondary electrons is not an important factor in their angular distributions. Given that the two electrons have equal energies it might be expected that a repulsive interaction should occur between them as they leave the collision region. The fact that we observe no such interaction may be due to the two-step nature of the Auger process resulting in sequential ejection of the two electrons.

The satellite Auger spectrum of Mg extends to about 60 eV, and there are several satellite lines close to 45 eV which potentially complicate our analysis. The intensities of these satellites (6% of the main Auger doublet, see Breuckmann *et al.* 1976 and Pejcev *et al.* 1977) are weak enough that their contribution can be neglected. For unequal secondary electrons the 35 eV Auger and ejected 2p electron are distinguishable. The measured cross section for the ejection of a 45 eV electron and emission of a 35 eV Auger electron is shown in Fig. 5. The cross section is once again plotted as a function of ω_{12} , the included angle. In addition the data are labelled according to the value of θ_1 , the angle of the ejected electron relative to the incident direction. The cross section is no longer a function of only the included angle and is large for ejection in the forward ($\theta_1 = 45^\circ$) or backward ($\theta_1 = 135^\circ$) directions and small for ejection at right angles

to the incident direction ($\theta_1 = 90^\circ$). This is consistent with the photoionisation measurements of Hausmann *et al.* (1988). Photoionisation is expected to be similar to the present electron-impact ionisation measurements because the momentum transfer is small and in the forward direction.

We have analysed our measured angular correlation between Auger and ejected electrons in terms of the formalism developed by Kabachnik (1992) to describe the equivalent photoionisation experiment, which assumes a two-step Auger process within an independent-particle approximation. An analysis of this formalism reveals that our measured cross sections can be parametrised in terms of the three asymmetry parameters β_1 , β_2 and β_{12} . The quantities β_1 and β_2 describe the angular distributions of the ejected and Auger electrons respectively in a non-coincidence experiment, and β_{12} is a measure of the angular correlation between the two electrons.

We have obtained values of the three β parameters from our measured cross sections using a multiple linear-regression analysis. For comparison we have also calculated β_1 and β_2 using a Herman-Skillman (Herman and Skillman 1963; Manson and Cooper 1968) central-potential calculation and a relativistic random-phase approximation calculation (Desmukh and Manson 1983). Within the two-step independent particle approximation β_{12} is simply equal to $\beta_1/3$ (Kabachnik 1992). The calculated values of the parameters and those obtained by fitting the data are in qualitative agreement. The experimental values of β_1 decrease with decreasing ejected-electron energy as predicted, but are somewhat smaller than the theoretical values. A similar observation was made in the photoionisation measurements of Hausmann *et al.* (1988). The experimental values of β_2 are found to be much smaller than β_1 , as predicted by theory and observed in the photoionisation experiment. Within the accuracy of our experiment we get $\beta_{12} = \beta_1/3$ as obtained from theory.

4. (e, (3-1)e) Measurements of Direct Double-ionisation

We have performed measurements of the direct-double ionisation cross section at incident energies of 1052 and 422 eV and a total ejected-electron energy of 200 eV shared equally between the two detected electrons (Ford *et al.* 1996, 1998). The choice of ejected-electron energies ensures that we observe direct ionisation rather than resonant Auger ionisation. In these measurements the primary electron analyser is not operated, and only two outgoing electrons are detected by the secondary analysers. The final-ion state is therefore not known.

Absolute values of the measured cross sections are calculated from the known values of the analyser acceptance solid angles and energy resolutions, and estimates of the electron beam and target dimensions and densities. They are intended only to indicate order of magnitude. Relative normalisation between different measurements is accurate to within approximately 20% and was achieved by measuring the 35 eV Auger cross section at the beginning and end of each experiment. This normalisation accounts for variations in the incident beam and target gas density.

Once again the data cannot be plotted in any simple way as a function of all three independent variables, the problem then becomes finding a suitable sub-set of variables which characterise the cross sections. One possible model is to consider that momentum is transferred directly from the incident electron to

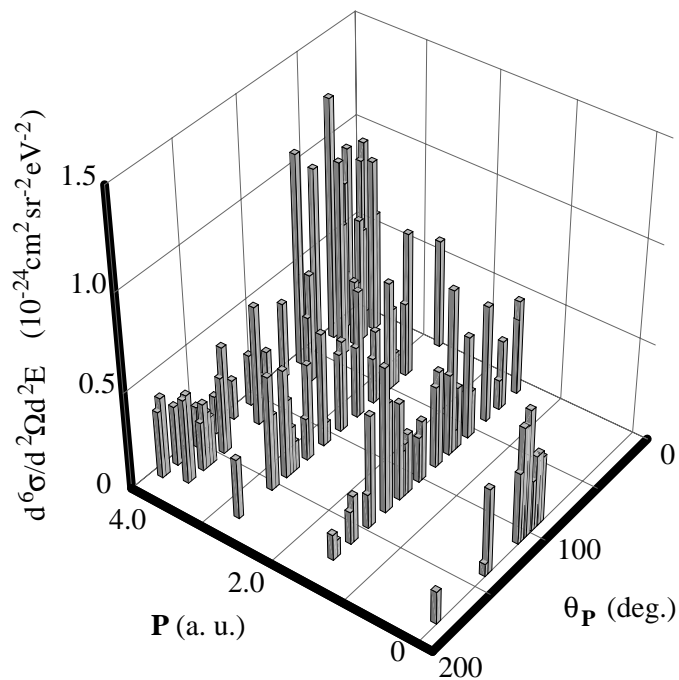


Fig. 6. Three-dimensional plot of the cross section for ejection of two 100 eV electrons at 1052 eV incident energy.

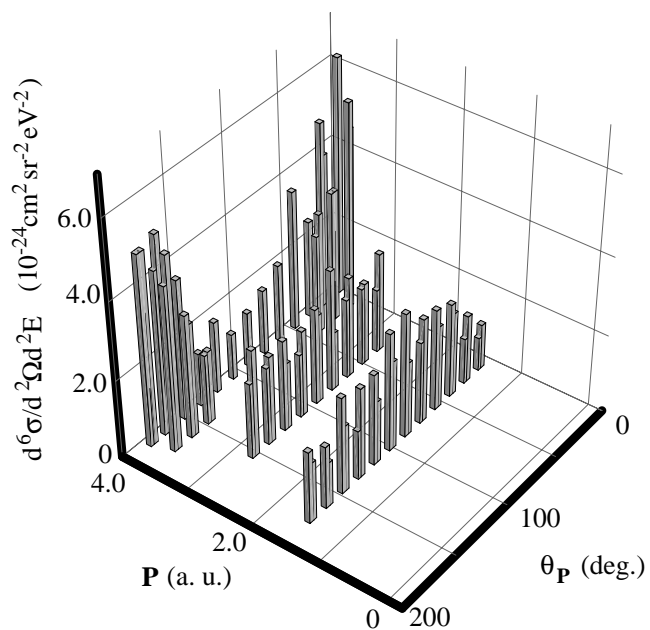


Fig. 7. Three-dimensional plot of the cross section for ejection of two 100 eV electrons at 422 eV incident energy.

a ‘single composite particle’ which is ejected with momentum $\mathbf{P} = \mathbf{p}_1 + \mathbf{p}_2$ and subsequently ‘decomposes’ to yield the two detected electrons. The cross section can then be plotted as a function of the magnitude $|\mathbf{P}|$ of the total momentum vector, and θ_P the angle between \mathbf{P} and the incident-electron direction; it must be remembered that a third independent variable [such as the rotational angle of the $(\mathbf{p}_1, \mathbf{p}_2)$ plane about \mathbf{P}] has been omitted. It is worth noting that constant $|\mathbf{P}|$ corresponds to a constant included angle ω_{12} between the two electrons.

The measured absolute differential cross section for an incident energy of 1052 eV is shown in the three-dimensional plot of Fig. 6 as a function of $|\mathbf{P}|$ and θ_P . At the maximum value of $|\mathbf{P}| = 3.83$ a.u., the cross section peaks in the forward direction around $\theta_P = 30^\circ$. Even at $\theta_P = 0^\circ$ the cross section is still relatively large, in which case we can deduce, from the energies of the final double-ion states and conservation of momentum that the final ion momentum must be at least 2.83 a.u. for the $3s^{-2}$ final ion state and 1.84 a.u. for the $2s^{-2}$ final state. More surprising is the small, but non-zero, amplitude at large θ_P where the final ion momentum must be very large (greater than 4.83 a.u. for $\theta_P = 180^\circ$).

Fig. 7 shows a similar plot of the cross section for an incident-electron energy of 422 eV. At $|\mathbf{P}| = 3.83$ a.u. the cross section peaks strongly in both the forward and backward directions with a deep minimum at $\theta_P = 90^\circ$. For backward ejection the final ion momentum must be extremely large since the momentum transfer cannot be in the backward direction. As the value of $|\mathbf{P}|$ decreases the minimum near $\theta_P = 90^\circ$ is replaced by a small maximum. At $|\mathbf{P}| = 1.47$ a.u., the net ejected-electron momentum is now smaller than the minimum possible momentum transfer (1.74 a.u. for production of the $3s^{-2}$ final state), and consequently at least a small amount of momentum must be transferred to the core.

We must now consider whether the cross sections are uniquely defined by only the two variables $|\mathbf{P}|$ and θ_P . The data of Figs 6 and 7 correspond to detection of the two electrons on opposite sides of the collision volume. For $|\mathbf{P}| = 3.83$ a.u. the included angle between the two electrons is $\omega_{12} = 90^\circ$, and for $\theta_P = 0^\circ$ (or 180°) $\mathbf{p}_0, \mathbf{p}_1$ and \mathbf{p}_2 are coplanar (i.e. all three vectors lie in the reference plane of Fig. 1), and the ejected-electron directions lie 45° (or 135°) on either side of the incident beam direction. As θ_P is swept from 0° to 180° , at a constant $|\mathbf{P}| = 3.83$ a.u., the $(\mathbf{p}_1, \mathbf{p}_2)$ plane rotates about an axis perpendicular to the incident-electron direction. At $\theta_P = 90^\circ$ this plane is perpendicular to the incident direction. By measuring the cross section in the ‘same-side’ mode we can additionally sample data points where $|\mathbf{P}| = 3.83$ a.u. and $\theta_P = 90^\circ$ as before, but now \mathbf{p}_1 and \mathbf{p}_2 are coplanar with \mathbf{p}_0 ; this corresponds to detection of both electrons in one analyser, one at an angle of 45° and the other at 135° to the incident direction. The effect of the orientation of the $(\mathbf{p}_1, \mathbf{p}_2)$ plane can be demonstrated by plotting both opposite and same-side data together as a function of the normalised absolute value of the scalar triple product, $|\mathbf{p}_1 \times \mathbf{p}_2 \cdot \mathbf{p}_0|$, for cases where the included angle is close to 90° . The normalised scalar triple product is zero if and only if the three vectors are coplanar, and approaches unity as the $(\mathbf{p}_1, \mathbf{p}_2)$ plane becomes perpendicular to the incident-electron direction. There is a clear difference between the 1052 eV data shown in Fig. 8 and the 422 eV data of Fig. 9. At 1052 eV there is no apparent correlation between the measured cross sections and the orientation of the $(\mathbf{p}_1, \mathbf{p}_2)$ plane. The 422 eV

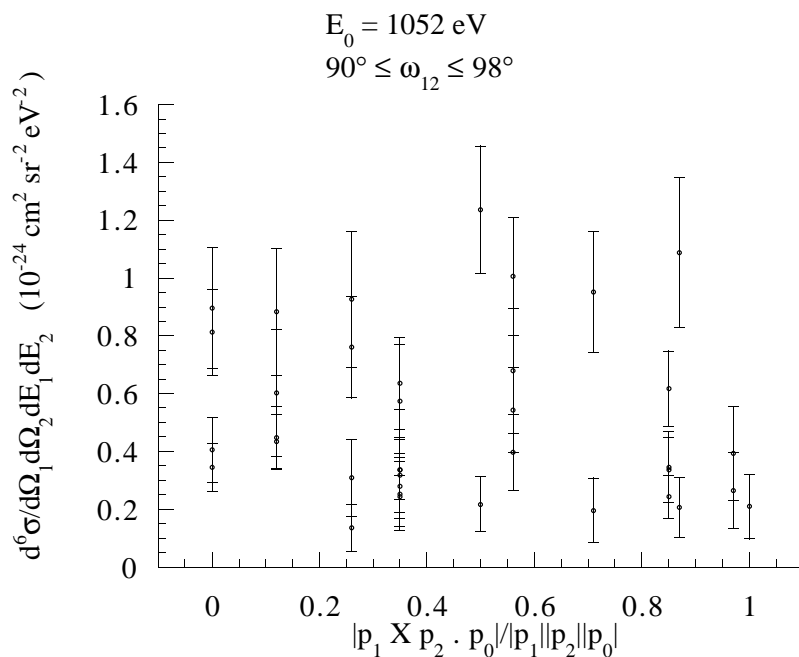


Fig. 8. Cross section for ejection of two 100 eV electrons at 1052 eV incident energy plotted as a function of the normalised absolute scalar triple product $|\mathbf{p}_1 \times \mathbf{p}_2 \cdot \mathbf{p}_0|$. Data are plotted for included angles $90^\circ \leq \omega_{12} \leq 98^\circ$.

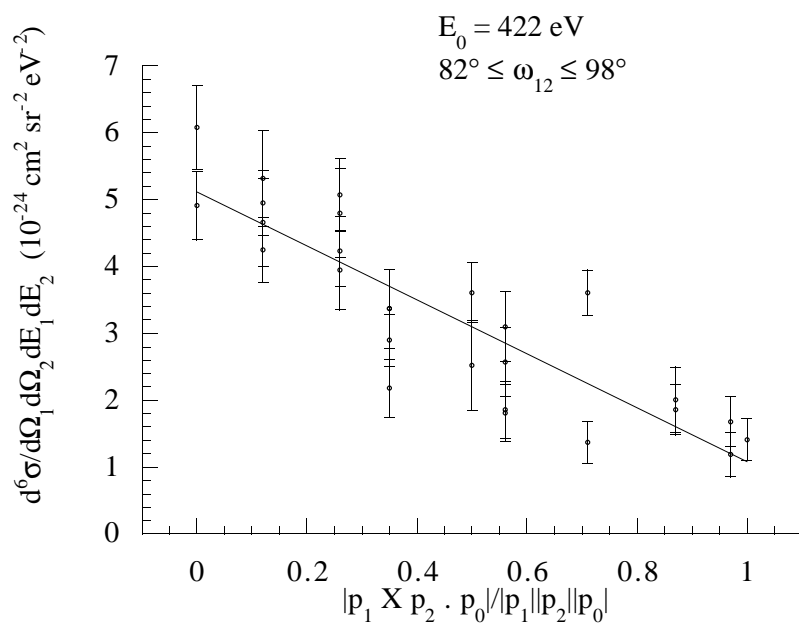


Fig. 9. Cross section for ejection of two 100 eV electrons at 422 eV incident energy plotted as a function of the normalised absolute scalar triple product $|\mathbf{p}_1 \times \mathbf{p}_2 \cdot \mathbf{p}_0|$. Data are plotted for included angles $82^\circ \leq \omega_{12} \leq 98^\circ$.

data, on the other hand, are inversely proportional to the orientation, showing a maximum when the three vectors lie in a common plane. The cross section for ejection of two electrons at right angles to each other and in a plane containing the incident direction is relatively insensitive to the value of θ_P ; the variation is less than a factor of two for $\theta_P = 0^\circ, 82^\circ, 90^\circ$ and 180° , compared with the variation of almost a factor of 5 associated with rotation of the $(\mathbf{p}_1, \mathbf{p}_2)$ plane.

5. Direct Double-ionisation Mechanisms

The simple composite-particle mechanism for double-ionisation provides an appealing explanation for ejection of the two electrons into the backward direction as being due to a reflection of the composite particle from the ion core. The corresponding effect is observed in single ionisation, but only at much lower incident energies. Our consideration of the effect of rotating the $(\mathbf{p}_1, \mathbf{p}_2)$ plane for the 422 eV data, as shown in Fig. 9, does not support this mechanism, however, since the cross section shows a strong dependence on the rotation of the plane around \mathbf{P} .

At incident energies of 422–1052 eV single ionisation with relatively large momentum transfer is well-described by a binary knockout (Lahmam-Bennani *et al.* 1991; Duguet and Lahmam-Bennani 1992). This mechanism has been extended to double-ionisation—the two step mechanisms in which electrons are ejected in discrete, sequential binary interactions—and predicts that ejected electrons appear only in the forward direction. These mechanisms do not account for our observation that the incident and ejected-electron momentum vectors tend to lie in a common plane, or the large amount of momentum transferred to the residual ion. In connection with this latter point it should be noted that Jagutzki *et al.* (1996) in ion-momentum measurements also reported that, unlike single ionisation, double ionisation involves collisions with large momentum transfers to the core.

A third mechanism is where one electron receives almost all the momentum transferred and the second is ‘shaken-off’ as the core relaxes to a state of the doubly-charged ion. We have performed calculations of the differential cross sections corresponding to those of Figs 6 and 7 within the first Born Approximation (Ford *et al.* 1998). The method of calculation was a modification of that used by Stehman *et al.* (personal communication). The calculations, shown in Fig. 10, qualitatively reproduce the peak in the cross section for a pair of electrons ejected in the forward direction with large net momentum and the shift of this peak to larger values of θ_P as the net momentum decreases. The calculations do not, however, reproduce any probability for backwards ejection of the electrons. It must be remembered, however, that the final-ion state is not known in the measured cross sections. The calculations of Fig. 10 are limited to double ionisation of the two 3s electrons although similar calculations for the ejection of two 2p electrons gave similar results. The calculated cross section as a function of momentum transfer \mathbf{K} is largest near $|\mathbf{K}| = 2.71$ a.u., the momentum of a single 100 eV electron, and is consistent with a model where one electron receives almost all the momentum transferred and the second is ‘shaken-off’. To test for this mechanism in our experimental data we performed a measurement at an incident energy of 522 eV, in which case a momentum transfer of magnitude 2.71 a.u., all to one electron, would direct that electron into a detector at $\theta_1 = 45^\circ$.

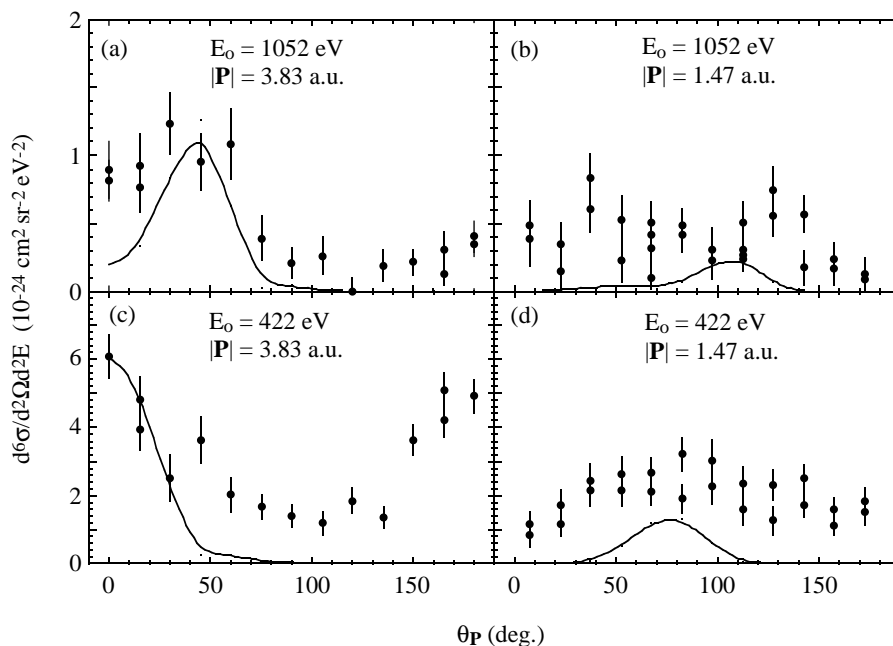


Fig. 10. Comparison between the measured differential cross section for ejection of two 100 eV electrons at incident energies of 1052 eV and 422 eV and a first Born approximation calculation based on a shake-off mechanism.

We then measured the coincidence rates between a detector at this angle and each of the other detectors. We would expect the angular distribution of the shake-off electron to be isotropic and so should measure the same coincidence rate between the various pairs of detectors. The result is in fact a variation of about a factor of 3.

It is possible that at 422 eV incident energy one of the detected electrons is the scattered electron. If the detected electrons are the scattered electron and a target electron ejected in a binary collision we would expect the incident electron momentum vector to lie in the same plane as these two electrons as observed in (e, 2e) single ionisation experiments. Backwards scattering or backwards ejection are not observed in single ionisation, however, when the incident energy is of the order of 400 eV and the momentum transfer exceeds 1 a.u. as is the case in the present experiments. At an incident energy of 1052 eV it is extremely unlikely that we detect the scattered electron since the energy loss would be too large.

6. Concluding Remarks

In the previous sections I have reviewed our recent experiments investigating the double-ionisation of magnesium. The results have been discussed in the context of double-ionisation mechanisms and compared with theoretical models.

For the case of resonant ionisation via the $L_{2,3}M_1M_1$ Auger process our (e, 3e) measurements show that there is a strong angular correlation between the ejected and Auger electron. The measured cross sections are comparable to those observed in photoionisation experiments and are well described by an independent-particle two-step Auger model. This is not surprising given that the

experiments have been conducted so that the momentum transfer and scattering angle of the incident electron are small. It would be interesting to extend these measurements to the satellite Auger spectrum of Mg which is relatively intense and indicates the degree of electron correlation present in the atom.

The results for direct double-ionisation indicate that the ionisation process changes considerably over the impact energy range employed, 400 eV to 1000 eV. A relatively high energy, 100 eV, has been chosen for the two detected electrons and, although the momentum transfer is not known, in all cases it must be at least as large as 1 a.u. At higher impact energies the collision ejects both electrons into the forward direction, although there is a small probability for backward ejection. At lower impact energies, forward and backward ejection become equally probable and there is a large probability for the two detected electrons to be ejected at right angles to each other in a plane that includes the incident electron momentum vector. None of the models of double-ionisation described provide a satisfactory explanation of these observations. Backward scattering implies penetration of the incident electron deep into the atom, suggesting significant participation by inner-shell electrons. The observed angular correlation between the detected electrons and the incident beam direction suggests an angular momentum conservation that is not described in existing models. Many of the questions raised in these experiments can only be answered by performing the full (e, 3e) measurement so that the final-ion state and momentum transfer are known. The spectrometer at University of Maryland is currently being modified in order to carry out this task. The primary analyser is being re-designed to increase its acceptance solid angle and thereby make measurement of the small direct double-ionisation cross sections a realistic proposition.

Acknowledgments

The author wishes to thank his co-workers at the University of Maryland and Johns Hopkins University, B. El-Marji, J. P. Doering, J. H. Moore, M. A. Coplan and J. W. Cooper. This research was supported by NSF grant No. PHY-91-07337 and PHY-95-15516. Additional support was provided by NATO Collaborative Research Grant No. CRG 920101 and by the University of Maryland.

References

- Breuckmann, B., Schmidt, V., and Schmitz, W. (1976). *J. Phys. B* **9**, 3037.
- Desmukh, P. C., and Manson, S. T. (1983). *Phys. Rev. A* **28**, 209.
- Duguet, A., and Lahmam-Bennani, A. (1992). *Z. Phys. D* **23**, 383.
- El-Marji, B., Duguet, A., Lahmam-Bennani, A., Lecas, M., and Wellenstein, H. F. (1996a). *J. Phys. B* **28**, L733.
- El-Marji, B., Lahmam-Bennani, A., Duguet, A., and Reddish, T. J. (1996b). *J. Phys. B* **29**, L157.
- Ford, M. J., Doering, J. P., Coplan, M. A., Cooper, J. W., and Moore, J. H. (1995a). *Phys. Rev. A* **51**, 418.
- Ford, M. J., Doering, J. P., Moore, J. H., and Coplan, M. A. (1995b). *Rev. Sci. Instrum.* **66**, 3137.
- Ford, M. J., El-Marji, B., Doering, J. P., Moore, J. H., Coplan, M. A., and Cooper, J. W. (1998). *Phys. Rev. A* **57**, 325.
- Ford, M. J., Moore, J. H., Coplan, M. A., Cooper, J. W., and Doering, J. P. (1996). *Phys. Rev. Lett.* **77**, 2650.
- Hausmann, A., Kammerling, B., Kossmann, H., and Schmidt, V. (1988). *Phys. Rev. Lett.* **61**, 2669.

- Herman, F., and Skillman, S. (1963). 'Atomic Structure Calculations' (Prentice-Hall: Englewood Cliffs, NJ).
- Inokuti, M. (1971). *Rev. Mod. Phys.* **43**, 297.
- Jagutzki, O., Speilberger, L., Dorner, R., Nuttgens, S., Mergel, V., Schmidt-Bocking, H., Ullrich, J., Olson, R. E., and Buck, U. (1996). *Z. Phys. D* **36**, 5.
- Kabachnik, N. M. (1992). *J. Phys. B* **25**, L369.
- Kammerling, B., and Schmidt, V. (1991). *Phys. Rev. Lett.* **67**, 1848.
- Lahmam-Bennani, A., and Duguet, A. (1991). Sixth Int. Symp. on Correlations and Polarisation in Electronic and Atomic Collisions, Flinders University, Adelaide.
- Lahmam-Bennani, A., Duguet, A., Grisogono, A. M., and Lecas, M. (1992). *J. Phys. B* **25**, 2873.
- Lahman-Bennani, A., Dupre, C., and Duguet, A. (1989). *Phys. Rev. Lett.* **63**, 1582.
- Lahmam-Bennani, A., Ehrhardt, H., Dupre, C., and Duguet, A. (1991). *J. Phys. B* **24**, 3645.
- Manson, S. T., and Cooper, J. W. (1968). *Phys. Rev. A* **165**, 165.
- Pascual, R., Mitroy, J., Frost, L., and Weigold, E. (1988). *J. Phys. B* **21**, 4239.
- Pejcev, V., Ottley, T. W., Rassi, D., and Ross, K. J. (1977). *J. Phys. B* **10**, 2389.
- Sandner, W., and Volkel, M. (1984). *J. Phys. B* **17**, L597.
- Sewell, E. C., and Crowe, A. (1984). *J. Phys. B* **17**, 2913.
- Stefani, G., Avaldi, L., Lahmam-Bennani, A., and Duguet, A. (1986). *J. Phys. B* **19**, 3787.

Manuscript received 30 January, accepted 6 March 1998